Principal component analysis of early immune cell dynamics during pembrolizumab treatment of advanced urothelial carcinoma

TARO TESHIMA[1,2], YUKARI KOBAYASHI[2], TAKETO KAWAI[1], YOSHIHIRO KUSHIHARA[2], KOJI NAGAOKA[2], JIMPEI MIYAKAWA[1], YOSHIYUKI AKIYAMA[1], YUTA YAMADA[1], YUSUKE SATO[1], DAISUKE YAMADA[1], NOBUYUKI TANAKA[3], TATSUHIKO TSUNODA[4,5], HARUKI KUME[1] and KAZUHIRO KAKIMI[2]

Departments of [1]Urology and [2]Immunotherapeutics, The University of Tokyo Hospital, Tokyo 113-8655; [3]Department of Urology, Keio University School of Medicine, Tokyo 160-8582; [4]Department of Biological Sciences, School of Science, The University of Tokyo, Tokyo 113-0033; [5]Laboratory for Medical Science Mathematics, RIKEN Center for Integrative Medical Sciences, Yokohama, Kanagawa 230-0045, Japan

Received March 2, 2022; Accepted May 12, 2022

DOI: 10.3892/ol.2022.13384

Abstract. Immune checkpoint inhibitors have been approved as second-line therapy for patients with advanced urothelial carcinoma (UC). However, which patients will obtain clinical benefit remains to be determined. To identify predictive biomarkers for the pembrolizumab (PEM) response early during treatment, the present study investigated 31 patients with chemotherapy-resistant recurrent or metastatic UC who received 200 mg PEM intravenously every 3 weeks. Blood was taken just before the first dose and again before the second dose, and the peripheral blood mononuclear cells of all 31 pairs of blood samples were immune phenotyped by flow cytometry. Data were assessed by principal component analysis (PCA), correlation analysis and Cox proportional hazards modeling in order to comprehensively determine the effects of PEM on peripheral mononuclear immune cells. Absolute counts of $CD45RA^+CD27^-CCR7^-$ terminally differentiated $CD8^+$ T cells and $KLRG1^+CD57^+$ senescent $CD8^+$ T cells were significantly increased after PEM administration (P=0.042 and P=0.043, respectively). Senescent and exhausted $CD4^+$ and $CD8^+$ T cell dynamics were strongly associated with each other. By contrast, counts of monocytic myeloid-derived suppressor cells (mMDSCs) were not associated with other immune cell phenotypes. The results of PCA and non-hierarchical clustering of patients suggested that excessive T cell senescence and differentiation early during treatment were not necessarily associated with a survival benefit. However, decreased mMDSC counts after PEM were associated with improved overall survival. In conclusion, early on-treatment peripheral T cell status was associated with response to PEM; however, it was not associated with clinical benefit. By contrast, decreased peripheral mMDSC counts did predict improved overall survival.

Introduction

The anti-PD-1 antibody pembrolizumab (PEM) is currently approved as second line therapy for cisplatin-resistant urothelial carcinoma (UC), but the objective response rate was only 21.1% (95% CI, 16.4 to 26.5) in the KEYNOTE-045 clinical trial (1). Therefore, it is important to find biomarkers to predict which patients will benefit from this drug and to identify factors that reflect its lack of therapeutic effect in UC patients. To this end, we investigated whether immune profiling could yield biomarkers for the early prediction of therapeutic effects in individual patients.

A commonly-used predictive biomarker of checkpoint inhibitor efficacy is the tumor mutational burden (TMB), an indirect indicator of tumor antigenicity resulting from mutations in the cancer cells. A positive correlation between log (TMB) and the mean response rate has been reported in a meta-analysis of 27 different cancers (2). Significant correlations between high TMB and response to the anti-PD-L1 antibody atezolizumab have been reported in patients with locally-advanced and metastatic UC after treatment with platinum-based chemotherapy (3). It has also been reported

Correspondence to: Professor Kazuhiro Kakimi, Department of Immunotherapeutics, The University of Tokyo Hospital, 7-3-1 Hongo, Bunkyo-Ku, Tokyo 113-8655, Japan
E-mail: kakimi@m.u-tokyo.ac.jp

Abbreviations: PEM, pembrolizumab; PBMC, peripheral blood mononuclear cell; CBC, complete blood count; TMB, tumor mutational burden; CRP, C-reactive protein; LDH, lactate dehydrogenase; mMDSC, monocytic myeloid-derived suppressor cell; OS, overall survival; UC, urothelial carcinoma; CM, central memory; EM, effector memory; TD, terminally differentiated; eTreg, effector regulatory T cell; G-CSF, granulocyte colony-stimulating factor; ICI, immune checkpoint inhibitor; PCA, principal component analysis

Key words: UC, anti-programmed cell death protein 1 therapy, PEM, eTreg, mMDSC, differentiation, exhaustion, senescence

that a high neutrophil-to-lymphocyte ratio in peripheral blood (PB) is associated with poorer responses to anti-PD-1 antibodies in patients with non-small cell lung cancer and melanoma (4). Other potential predictive biomarkers for the efficacy of immune checkpoint inhibitors (ICIs) include C-reactive protein (CRP) and Lactate Dehydrogenase (LDH). In a retrospective study, baseline elevated CRP was an independent predictor of worse progression-free survival (PFS), worse overall survival (OS) and a lower overall response rate (ORR) in patients treated with PD-1/PD-L1 ICIs (5). Baseline low serum LDH, high eosinophil counts and high lymphocyte counts were independent prognostic factors for PD-1 benefit in patients with advanced melanoma (6). In addition, it has been reported that phenotypes of inflammatory cells in PB influence PD-1 ICI prognosis in non-small cell lung cancer; these included higher baseline $CD62L^{low}CD4^+$ T cells and lower $CD25^+FOXP3^+CD4^+$ T cells (7) and higher $PD\text{-}1^+CD8^+$ T cells and NK cells (8). Notably, levels of myeloid-derived suppressor cells (MDSC) in PB and tissues have been reported as poor prognostic factors in UC (9). However, the dynamics of individual immune cells and their phenotypes after PEM treatment and associations with response or resistance to PEM have not yet been explored.

In order to understand the dynamics of immune cells and their phenotypes in early on-treatment samples, we evaluated PB mononuclear cells (PBMCs) before and after the first administration of PEM. We applied principal component analysis (PCA) on immune profile data for different immune cells in order to evaluate the immunological changes resulting from PEM administration. Finally, we investigated whether immune profiling could provide biomarkers for the early prediction of individual therapeutic effects.

Materials and methods

Patients. This clinical study analyzed the immunological impact of the anti-PD-1 antibody PEM on chemotherapy-resistant recurrent and metastatic UC patients at the University of Tokyo Hospital. The research protocol was approved by the Ethical Committee of The University of Tokyo [approval no. 3652-(6)] and written informed consent was obtained from each patient before they entered the study. All procedures in the present study were performed according to the ethical standards of the institution and were in conformity with the 1964 Helsinki Declaration and its later amendments, or comparable ethical standards. Thirty-one chemotherapy-resistant advanced UC patients were recruited from May 2018 to May 2020 (Table I).

Treatment. Patients received 200 mg of PEM intravenously every 3 weeks. Blood was collected just before the first and again just before the second administration of PEM. The first dose was given in the hospital, and the second dose was administered in the outpatient chemotherapy room. The schedule of the second dose and the timing of blood sampling were delayed in some patients, resulting in the interval between the first and second dose ranging from 17 to 29 days (Fig. S1). However, these differences in the timing of dosing did not affect the immunological parameters used in this study (Table SI). Therefore, all 31 patients' data were accepted for the analysis.

PBMC isolation and flow cytometry. PBMCs were isolated from peripheral venous blood by density gradient centrifugation at 1,100 x g for 20 min at room temperature using Lymphoprep™ (cat. no. 1114547; Alere Technologies AS) and were then cryopreserved in Bambanker™ freezing medium (cat. no. CS-02-001; 01; Nippon Genetics Co., Ltd.). Cryopreserved PBMCs were thawed in RPMI-1640 (cat. no. 189-02025; Wako Pure Chemical Industries, Ltd.) supplemented with 50 IU/ml Benzonase® Nuclease (cat. no. E1014; Sigma-Aldrich; Merck KGaA). Cells ($1x10^6$) were stained in 100 μl phosphate-buffered saline containing 1% FBS (cat. no. 17012; Sigma-Aldrich; Merck KGaA) and 0.1% sodium azide (cat. no. 195-11092; Wako Pure Chemical Industries, Ltd.) using a 1:100 dilution of the antibodies (Abs) listed in Table SII. Dead cells were excluded by staining using Zombie Yellow™ Fixable Viability kits (cat. no. 423104; BioLegend, Inc.). For surface staining, cells were incubated with the Abs at 4˚C in the dark for 30 min. Cells were fixed in 0.5% paraformaldehyde for nuclear staining before data acquisition and incubated with mAbs at room temperature in the dark for 45 min. Flow cytometry was performed on a CytoFLEXS (Beckman Coulter, Inc.) and data were analyzed by FlowJo™ v10 software (TreeStar) (Fig. S2). The gating strategies for $CD4^+$ and $CD8^+$ T cells were based on their expression of CD45RA, CD27 and CCR7, as reported by Jones *et al* (10). Monocytic myeloid-derived suppressor cells (mMDSCs) were defined as $CD11b^+CD14^+HLA\text{-}DR^{-/low}CD15^-CD33^+$, based on the strategy of Bronte *et al* (11). The gating for regulatory T cells (Treg) was set based on the analysis reported by Miyara *et al* (12), i.e., FOXP3-high cells based on $FOXP3^+Ki67^+CD45RA^-CD4^+$ staining were considered effector Treg (eTreg).

Absolute counts of immune cells. Absolute counts of each immune cell fraction were calculated by multiplying the percentage of each in PBMC and the sum of lymphocyte and monocyte counts in whole blood. The degree of change was calculated by subtracting the absolute counts before PEM administration from those after PEM administration.

Transcriptome analysis. To analyze IMvigor210 (NCT02108652) data, the expression data and clinical data were obtained from IMvigor 210 Core Biologies (http://research-pub.gene.com/IMvigor210CoreBiologies). We then ran ssGSEA (13), using gene-sets for MDSC (14) and tumor-associated macrophages (TAM) (15).

Statistical analysis. All statistical analyses were performed using R Statistical Software (version 4.1.0; R Foundation for Statistical Computing, Vienna, Austria) and installed R packages. Data were analyzed using the Wilcoxon signed-rank test when comparing two groups between each set of matched pairs with the R software package 'exactRankTests' (version 0.8-34). Data were analyzed using the Mann-Whitney test when comparing two independent groups with the R default installed package. The Kruskal-Wallis test was used to compare three or more independent groups for non-parametric data with the R default package. For post-hoc analysis, Steel-Dwass test was performed with the R software package 'NSM3' (version 1.16). Spearman's

Table I. Characteristics of patients with UC treated with pembrolizumab.

Characteristics	Value (n=31)
Patient age, years	
Median	70
Range	26-80
Male, n (%)	23 (74.2)
Ex-smoker, n (%)	19 (61.3)
Number of previous chemotherapy cycles	
Median	3
Range (1stQ, 3rdQ)	1-21 (3, 5)
Primary tumor, n (%)	
BC	10 (32.3)
Upper UC	16 (51.6)
BC and upper UC	5 (16.1)
TNM staging, n (%)	
0	1 (3.2)
I	5 (16.1)
II	1 (3.2)
III	20 (64.5)
IV	4 (12.9)
Numbers of visceral metastases before pembrolizumab, n (%)	
1	17 (54.8)
2	11 (35.5)
3	3 (9.7)
Chemotherapy regimen before pembrolizumab, n (%)	
DDMVAC	5 (16.1)
GC	11 (35.5)
GCa	13 (41.9)
Others	2 (6.5)

1stQ, first quartile; 3rdQ, third quartile; UC, urothelial carcinoma; BC, bladder cancer; DDMVAC, dose-dense MVAC, methotrexate, vinblastine, adriamycin, and cisplatin; GC, gemcitabine and cisplatin; GCa, gemcitabine and carboplatin.

rank correlation coefficient analysis was used to analyze the correlation with the R default installed package. A Cox proportional hazards model was used in the univariate analyses of overall survival with the R software package 'survival' (version 3.2-13). Kaplan-Meier estimation of survival of patients with high or low mMDSC levels by log-rank testing used the R software package 'survival' (version 3.2-13). The degree of change of each immune cell subset after PEM was analyzed using a multivariate PCA with the R software package 'factoextra' (version 1.0.7). Data were visualized with the R software package 'ggplot2' (version 3.3.5), 'survminer' (version 0.4.9), and 'corrplot' (version 0.92). $P<0.05$ was considered to indicate a statistically significant difference.

Results

Changes in complete blood count (CBC) and immune cells associated with PEM treatment. To identify predictive biomarkers for the outcome of PEM treatment of UC, we focused on pre-treatment and early on-treatment blood samples. First, to determine which parameters in CBC were significantly changed after the initial dose of PEM, each item of laboratory data was compared before and after its administration. We found that hemoglobin was significantly increased 3 weeks after starting PEM ($P<0.001$; Fig. 1, Table SIII). It is likely that hemoglobin values improved with the recovery of hematopoietic capacity because of the cessation of chemotherapy. Increases and decreases in white blood cells, platelets, neutrophils, lymphocytes and monocytes varied from patient to patient with no overall recognizable pattern.

Next, PBMCs were phenotyped by flow cytometry (Figs. S2 and 2). Three weeks after the initial dose of PEM, the absolute numbers of PD-1$^+$CD57$^-$CD4$^+$ T cells and PD-1$^+$CD57$^-$CD8$^+$ T cells were significantly decreased ($P<0.001$, $P=0.002$, respectively; Fig. 2, Table SIV). On the other hand, PD-1$^-$CD57$^+$CD4$^+$ T cell and PD-1$^-$CD57$^+$CD8$^+$ T cell numbers were significantly increased ($P<0.001$, $P=0.008$, respectively). The decrease of PD-1$^+$ cells and increased PD-1$^-$ cells were artifacts caused by the competition of binding to PD-1 between PEM and the detection antibody, clone EH12.2H7 (16). Therefore, except for pre-treatment samples, we removed the data containing PD-1 staining from further analyses. CD45RA$^+$CD27$^-$CCR7$^-$ terminally differentiated (TD) CD8$^+$ T cells and KLRG1$^+$CD57$^+$ senescent CD8$^+$ T cells were significantly increased ($P=0.042$ and $P=0.043$, respectively). Thus, the profile of CD8$^+$ T cells in PB shifted towards a more differentiated and senescent signature after PEM. In addition, eTregs significantly decreased ($P=0.015$; Fig. 2 and Table SIV).

Next, we investigated whether these changes induced by PEM affected the prognosis of UC patients. Univariate analysis with Cox regression did not show any significant prognostic relevance of the changes in CBC and different immune cell counts before and after PEM treatment (Tables SV and SVI).

Integrated analysis of immunophenotypic changes in PBMC. To integrate these changes in immune cells following PEM treatment into a representation of the dynamics of the immune system, changes in the different immune cell subsets were comprehensively analyzed by PCA (Fig. 3 and Table SVII). First, changes in cell counts for each immune cell phenotype before and after PEM were calculated and entered into the PCA. Next, the changes were plotted in the first two principal component spaces (Fig. 3A). This showed that CD4$^+$ and CD8$^+$T cells with effector memory (EM), TD, and senescent phenotypes clustered closely around the first principal component (PC1). Similarly, CD4$^+$ and CD8$^+$ T cells with naïve and central memory (CM) phenotypes clustered more around PC2. On the other hand, the contribution of eTregs and mMDSCs was limited (Table SVII).

Individual patient data were plotted based on the variable correlations of changes in immune cell fractions after PEM (Fig. 3B). The patients were divided non-hierarchically into three groups by k-means clustering, i.e., cluster 1 (PC1 side), cluster 2 (PC2 side), and cluster 3 (the opposite side of PC1 and

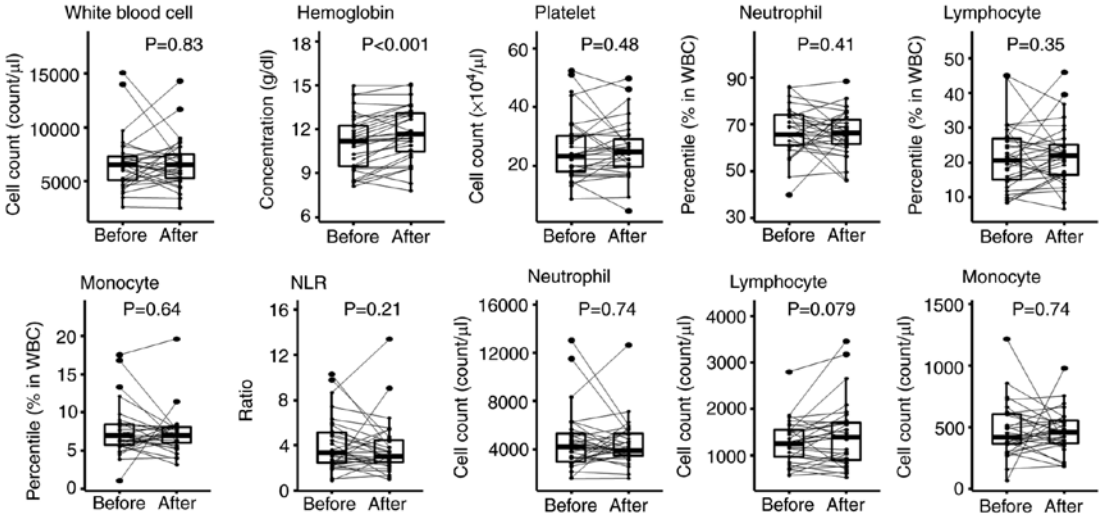

Figure 1. Hematological changes after PEM administration, comparing complete blood count just before PEM administration and 3 weeks thereafter using the Wilcoxon signed-rank test. Only the hemoglobin concentration was significantly elevated after PEM administration. NLR, neutrophil-to-lymphocyte ratio; PEM, pembrolizumab; WBC, white blood cell.

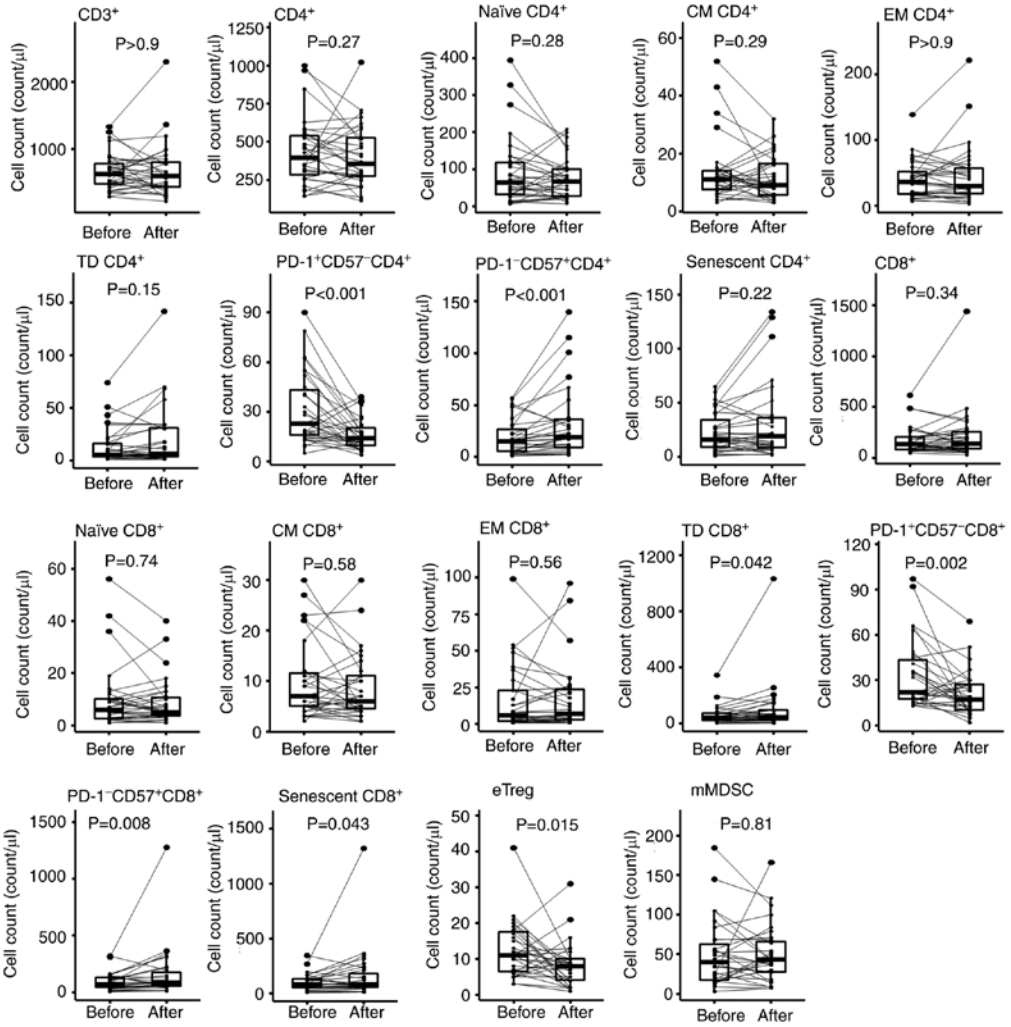

Figure 2. Changes in immune cells after PEM treatment. To investigate the changes in immune cells following PEM administration, a comparison was made between the absolute counts in each immune cell fraction of PBMCs just before PEM administration and 3 weeks thereafter using the Wilcoxon signed-rank test. Absolute cell counts were calculated by multiplying the percentages of each immune cell fraction and the PBMC counts; PBMC counts were calculated by the sum of lymphocyte counts and the monocyte counts in whole blood cells. Naïve, $CD45RA^{+}CD27^{+}CCR7^{+}$; CM, central memory ($CD45RA^{-}CD27^{+}CCR7^{+}$); EM, effector memory ($CD45RA^{-}CD27^{-}CCR7^{-}$); TD, terminally differentiated ($CD45RA^{+}CD27^{-}CCR7^{-}$); eTreg, effector regulatory T cell ($FOXP3^{high}CD45RA^{-}CD4^{+}$ T cell); mMDSC, monocytic myeloid-derived suppressor cell ($CD11b^{+}CD14^{+}CD15^{-}HLA\text{-}DR^{-}CD33^{+}$); PBMC, peripheral blood mononuclear cell; PD-1, programmed cell death protein 1; PEM, pembrolizumab.

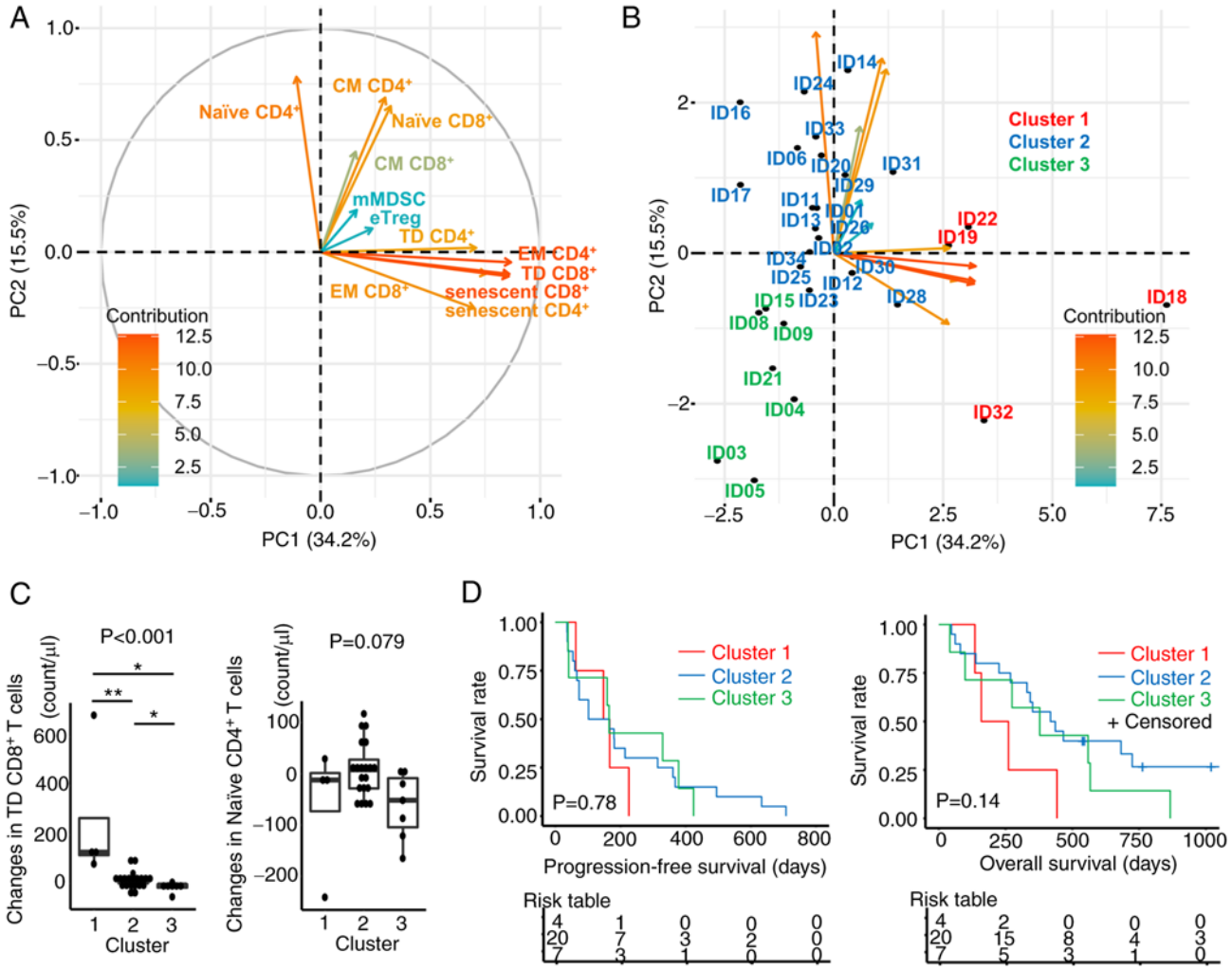

Figure 3. PCA of changes in immune cells after PEM treatment. (A) Correlation plots in PCA were constructed to examine the changes of each immune cell phenotype in PBMCs. The absolute counts of each immune cell fraction were calculated by multiplying the percentages of each fraction and the PBMC counts; PBMC counts were determined by the sum of lymphocyte counts and the monocyte counts from the routine clinical laboratory data. The changes were calculated by subtracting the values before PEM administration from those after PEM administration. Vectors indicate the increase of the respective changes in immune cells. The color is defined by the contribution of variables for the first two principal components. (B) Plots for individual patients were loaded on the respective principal components. The patients were divided into three groups by the k-means method using the first and second principal components. (C) Changes in TD CD8$^+$ T cells and naïve CD4$^+$ T cells were compared in these three clusters. Kruskal-Wallis test was performed and the P-value was indicated on the top of the panel. For post-hoc analysis, Steel-Dwass test was performed: *P<0.05, **P<0.01. (D) Kaplan-Meier estimates of progression-free survival and overall survival according to three clusters based on the results of PCA. A log-rank test was performed. naïve, CD45RA$^+$CD27$^+$CCR7$^+$; CM, central memory (CD45RA$^-$CD27$^+$CCR7$^+$); EM, effector memory (CD45RA$^-$CD27$^-$CCR7$^-$); TD, terminally differentiated (CD45RA$^+$CD27$^-$CCR7$^-$); eTreg, effector regulatory T cell (FOXP3^{high}CD45RA$^-$CD4$^+$ T cell); mMDSC, monocytic myeloid-derived suppressor cell (CD11b$^+$CD14$^+$CD15$^-$HLA-DR$^-$CD33$^+$); PBMC, peripheral blood mononuclear cell; PC1, the first principal component; PC2, the second principal component; PCA, principal component analysis; PEM, pembrolizumab.

PC2). The number of clusters 3 in k-means was determined using the R package 'NbClust' (version 3.0). This approach revealed that changes of TD CD8$^+$ T cells were significantly greater in cluster 1 (P<0.001) and changes of naïve CD4$^+$ T cells tended to be greater in cluster 2 (P=0.079) (Fig. 3C). Next, we compared PFS and OS from the initiation of PEM administration in these three clusters to determine whether these commonly recognized changes in PB immune cells were associated with prognosis (Fig. 3D). This approach showed that patients in cluster 1 had a relatively poor prognosis, whereas those in cluster 3 tended to have a better prognosis, but these differences did not reach statistical significance in terms of OS and PFS (P=0.14, P=0.78, respectively). These results suggest that T cell activation is needed for a response, but excessive activation and differentiation of T cells might not increase patient survival. Thus, inhibition of senescence and excessive differentiation of effector cells during PEM treatment might help sustain the effect of immunotherapy over an extended period, leading to a better prognosis.

Relationships between immune cell phenotypes. To investigate the relationships between immune cells from different PCA directions, correlation coefficients were calculated and verified together with the results of PCA. As shown in Fig. 4, components in the same axial direction with a strong contribution in Fig. 3 and Table SVII also correlate closely with each other. For example, TD CD8$^+$ T cells were well correlated with EM CD4$^+$ T cells (r=0.69), TD CD4$^+$ T cells (r=0.62) and senescent CD4$^+$ T cells (r=0.43). Senescent CD8$^+$ T cells were well correlated with EM CD4$^+$ T cells (r=0.69), TD CD4$^+$

	Naïve CD4⁺	CM CD4⁺	EM CD4⁺	TD CD4⁺	senescent CD4⁺	Naïve CD8⁺	CM CD8⁺	EM CD8⁺	TD CD8⁺	senescent CD8⁺	eTreg	mMDSC
Naïve CD4⁺	**1.00**											
CM CD4⁺	**0.43**	**1.00**										
EM CD4⁺	-0.05	0.12	**1.00**									
TD CD4⁺	0.10	0.27	**0.64**	**1.00**								
senescent CD4⁺	-0.06	0.15	**0.62**	**0.42**	**1.00**							
Naïve CD8⁺	**0.50**	**0.53**	0.17	0.26	0.03	**1.00**						
CM CD8⁺	0.12	0.22	**0.40**	0.11	0.21	0.23	**1.00**					
EM CD8⁺	-0.20	0.05	**0.66**	**0.42**	0.39	0.17	0.23	**1.00**				
TD CD8⁺	-0.06	0.12	**0.69**	**0.62**	**0.43**	**0.44**	0.21	**0.59**	**1.00**			
senescent CD8⁺	0.01	0.25	**0.69**	**0.58**	**0.65**	0.33	**0.41**	**0.64**	**0.80**	**1.00**		
eTreg	-0.02	0.14	0.32	0.12	0.18	0.16	**0.40**	0.37	0.27	**0.41**	**1.00**	
mMDSC	0.00	0.10	0.12	0.05	-0.06	0.06	0.17	0.22	0.29	0.24	**0.40**	**1.00**

Figure 4. Correlation coefficient analysis of immune phenotypes. Correlations between immune cell phenotypes in PBMCs were analyzed according to their changes in absolute cell counts before and after PEM administration. The absolute counts of each immune cell fraction were calculated by multiplying the percentages of each fraction and the PBMC counts; PBMC counts were determined by the sum of lymphocyte counts and the monocyte counts in the laboratory data. Changes were calculated by subtracting the values before PEM administration from those after PEM administration. naïve, $CD45RA^{+}CD27^{+}CCR7^{+}$; CM, central memory ($CD45RA^{-}CD27^{+}CCR7^{+}$); EM, effector memory ($CD45RA^{-}CD27^{-}CCR7^{-}$); TD, terminally differentiated ($CD45RA^{+}CD27^{-}CCR7^{-}$); eTreg, effector regulatory T cell ($FOXP3^{high}CD45RA^{-}CD4^{+}$ T cell); mMDSC, monocytic myeloid-derived suppressor cell ($CD11b^{+}CD14^{+}CD15^{-}HLA\text{-}DR^{-}CD33^{+}$); PBMC, peripheral blood mononuclear cell; PEM, pembrolizumab.

T cells (r=0.58), senescent $CD4^{+}$ T ells (r=0.65), EM $CD8^{+}$ T cells (r=0.64) and TD $CD8^{+}$ T cells (r=0.80). Conversely, eTregs and mMDSCs had notably lower coordinates and contributions to PC1 and PC2 (Table SVII). The absolute values of the correlation coefficients of mMDSCs with other immune cell fractions were all <0.3 except for eTregs with which mMDSCs had a weak correlation with a correlation coefficient of only 0.4 (Fig. 4). Therefore, we considered that eTregs and mMDSCs were not affected by PEM treatment and behave relatively independently from other immune cells on PEM treatment.

Impact of mMDSCs and eTregs on prognosis. The T cell compartment moved in the direction of differentiation and senescence even after only a single dose of PEM. These results are consistent with the expected mode of action of PEM. Therefore, to investigate whether the changes of mMDSCs, that were not associated with T cell changes, determined the clinical outcomes of UC patients receiving PEM, survival analysis was performed for patients with increased or decreased mMDSCs on treatment. This revealed that patients with decreased mMDSCs after PEM had significantly longer OS (P=0.049, Fig. 5A). In addition, the association between Treg dynamics following PEM treatment and patient survival was examined (Fig. 5D-F). Patients with increased eTregs also tended to enjoy better OS than those with decreased eTregs, although this was also not statistically significant (P=0.12, Fig. 5D). These changes in mMDSCs and eTregs were not associated with PFS or response to PEM (Fig. 5B, C, E and F).

Because the changes in mMDSC count were associated with OS after PEM, we compared clinical and laboratory data between patients with increased vs. decreased mMDSCs after PEM. Those patients with increased mMDSCs had received more cycles of chemotherapy before PEM treatment than patients with decreased mMDSCs (Table SVIII). However, there were no statistically significant differences in the changes of immune cells, especially T cells, before and after PEM between patients who received >6 courses of chemotherapy vs. those who received ≤6 courses (Table SIX). Although patients who received fewer chemotherapy courses did not necessarily exhibit decreased mMDSC counts after PEM, patients who did have decreased mMDSC had all received fewer courses (Fig. S3). Thus, taken together, these data suggest that pre-treatment chemotherapy influenced mMDSC but not T cell dynamics on PEM treatment.

Peripheral blood might not represent the tumor microenvironment in the advanced tumor. To compensate for this limitation, we re-analyzed the RNA-Seq data of pre-treatment tumor samples from a large phase 2 trial (IMvigor210) (17). ssGSEA using gene-sets for MDSC (14) and TAM (15) was performed in the IMvigor210 cohort. Patients were divided into two groups, High and Low, according to the median ssGSEA score of each gene set. None of them had a statistically significant influence on OS (Fig. S4). The immunological status might be different between PB and the tumor.

Discussion

In the present study, we performed immune profiling just before and 3 weeks after administration of PEM using PBMCs from 31 advanced UC patients refractory to chemotherapy. PEM promoted the accumulation of senescent and late-differentiated $CD8^{+}$T cells and reduced eTreg cell numbers in peripheral blood. PCA and correlation coefficient analysis demonstrated that the dynamics of senescent and late-differentiated $CD4^{+}$ and $CD8^{+}$ T cells were strongly associated with each other.

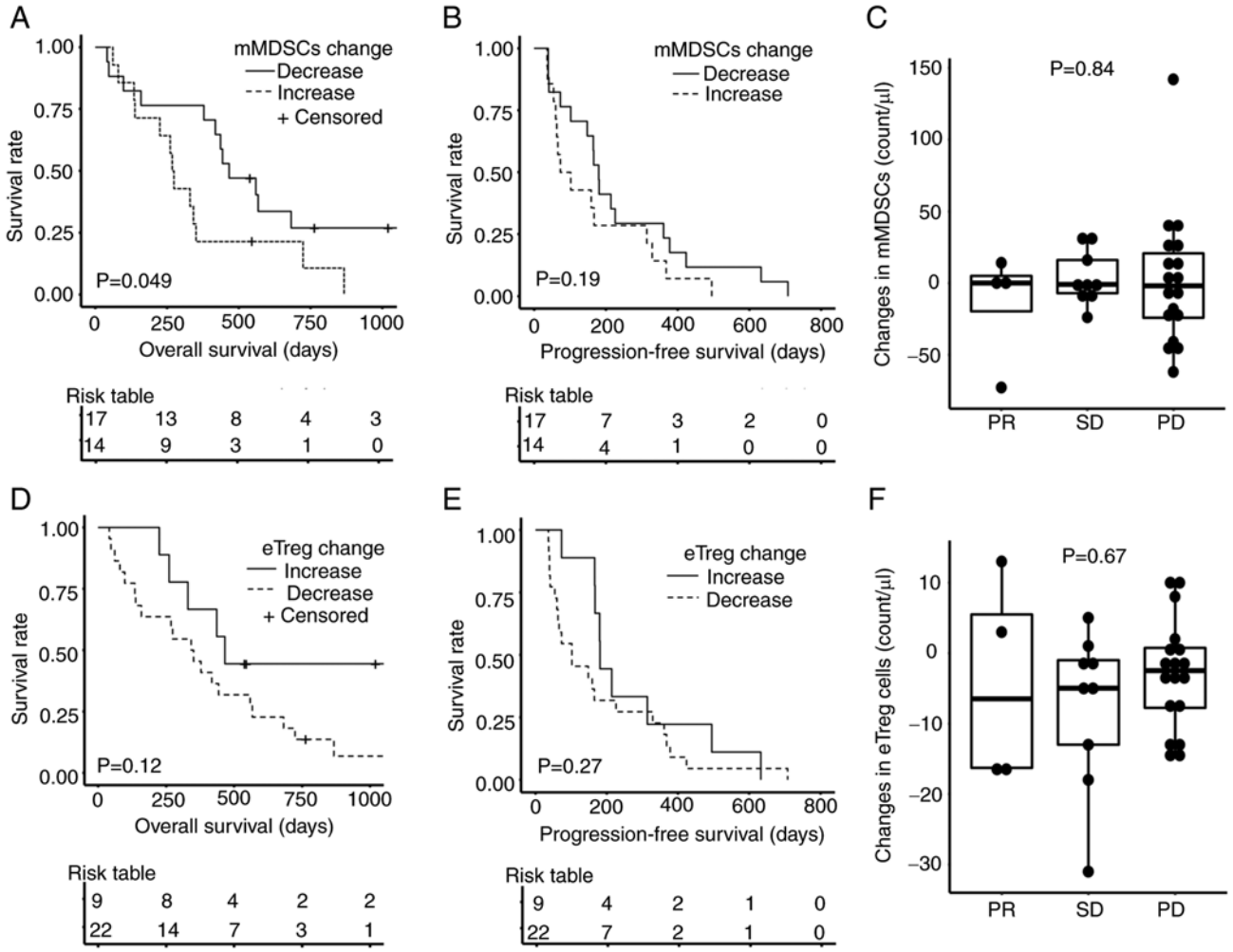

Figure 5. Overall survival, progression-free survival and responses to PEM according to the changes in mMDSCs and eTregs after PEM. Kaplan-Meier estimates of (A) overall survival and (B) progression-free survival according to the changes in mMDSCs. Increase, group with increased mMDSCs after PEM administration; decrease, group with decreased mMDSCs after PEM administration. (C) Changes in mMDSC counts were compared according to response to PEM. Kaplan-Meier estimates of (D) overall survival and (E) progression-free survival according to the changes in eTregs. Increase, group with increased eTreg after PEM administration; decrease, group with decreased eTreg after PEM administration; (F) Changes in eTreg counts were compared according to response to PEM. A log-rank test was performed in (A, B, D and E). Kruskal-Wallis test was performed in (C and F). eTreg, effector regulatory T cell ($FOXP3^{high}CD45RA^{-}CD4^{+}$ T cell); mMDSC, monocytic myeloid-derived suppressor cell ($CD11b^{+}CD14^{+}CD15^{-}HLA\text{-}DR^{-}CD33^{+}$); PEM, pembrolizumab; PR, partial response; SD, stable disease; PD, progressive disease.

Although mMDSCs did not show a unified tendency in patients and exhibited little correlation with other immune cell phenotypes, decreased mMDSC counts after PEM were associated with better overall survival.

This study demonstrated that PEM treatment was associated with increased numbers of $CD8^{+}$ T cells carrying senescence and terminal differentiation markers in most patients' peripheral blood (Fig. 2). Consistent with this, the contributions of both senescent and TD $CD8^{+}$ T cells to the first principal component in PCA were high (senescent $CD8^{+}$ T cells, PC1=0.86, TD $CD8^{+}$ T cells, contribution=0.86, Fig. 3A and Table SVII). Tumor-specific $CD8^{+}$ T cells may become dysfunctional, senescent, or terminally differentiated due to repeated antigen stimulation (18-20), and these cells have low proliferation capacity. Therefore, these dysfunctional cells may not exert a sufficient antitumor effect by themselves *in vivo* (21). These data may explain why patients in cluster 1 had shorter OS than patients in clusters 2 and 3 (Fig. 3D).

Peripheral eTreg counts were significantly decreased by PEM (Fig. 2). eTregs had a weak negative correlation with naïve $CD4^{+}$ T cells (Fig. 4). A previous study had reported that PD-L1 played an important role in differentiating naïve T cells into Tregs in experiments using PD-L1 knockout mice (22). PEM might inhibit eTreg differentiation, thereby increasing naïve $CD4^{+}$ T cells and decreasing eTreg after PEM. In addition, eTregs positively correlated with CM and senescent $CD8^{+}$ T cells (r=0.40 and 0.41, respectively, Fig. 4). Although not statistically significant, patients with increased eTreg displayed better OS (Fig. 5D). The presence of eTregs might limit the excessive differentiation of T cells induced by PEM. In contrast, there was no clear tendency regarding mMDSC changes before and after PEM when examining the whole patient cohort, and mMDSC after PEM behaved independently of other immune cells (Figs. 3 and 4). However, increased mMDSCs were associated with shorter OS (Fig. 5). This is consistent with a previous report that increased peripheral MDSCs were associated with unfavorable prognostic changes (23). As one

of the mechanisms of resistance to nivolumab, a previous study reported that mMDSCs expressing galectin-9 reduced the ability of TIM-3$^+$CD8$^+$ T cells in PBMCs of NSCLC patients to secrete IFNγ (24). mMDSC might have affected the CD8$^+$T cells described in the present study through this mechanism. However, we did not confirm the expression of either TIM3 or galectin-9 in our study.

Human MDSCs are commonly defined by the myeloid markers CD14$^+$, CD11b$^+$, and CD33$^+$, low HLA-DR and negativity for lineage markers (CD3, CD19 and CD56). These markers define three subsets of human MDSC, namely, monocytic MDSC (Lin$^-$HLA-DR$^{low/+}$CD11b$^+$CD33$^+$CD14$^+$), granulocytic or polymorphonuclear MDSC (CD11b$^+$CD14$^-$CD15$^+$ or CD11b$^+$CD14$^-$CD66b$^+$), and early-stage MDSC (HLA-DR$^-$CD33$^+$) (25). MDSCs are thought to represent an adverse prognostic factor in immunotherapy because they act suppressively in the immune microenvironment through direct cell-cell contact or indirect effects via remodeling the microenvironment. However, which subtypes of MDSCs are most prognostic is still controversial and may differ depending on the type of cancer (26). Unfortunately, density gradient purification of PBMCs from whole blood results in the loss of granulocytes. Therefore, our study could not examine granulocytic MDSCs. However, mMDSCs did clearly impact the prognosis of patients treated with PEM in our study (Fig. 5).

Chemotherapy before immunotherapy is a factor that can affect MDSCs. For example, gemcitabine and 5-FU selectively induce apoptotic cell death of MDSCs and increase IFN-γ production by tumor-infiltrating tumor-specific CD8$^+$T cells in *in vitro* and *in vivo* experiments in mice (27). However, even if the same chemotherapeutic agents are used, the effects on MDSCs may differ according to the dose or number of doses of chemotherapy (28). The duration, dose, and type of chemotherapy before immunotherapy were not standardized in the present study. However, granulocyte colony-stimulating factor (G-CSF) that affects MDSCs always followed chemotherapy in these patients. G-CSF promotes the survival of granulocytes, the proliferation and migration of neutrophils and, in addition, MDSCs (29). Therefore, the use of G-CSF for neutropenia, which occurs as an adverse event of chemotherapy, may contribute to the maintenance of MDSCs in the tumor microenvironment and diminish the effectiveness of subsequent immunotherapy.

Several molecules can be targeted to improve immune checkpoint inhibition by regulating MDSCs. A previous study with murine rhabdomyosarcoma showed that CXCR2-positive MDSCs inhibited the antitumor effect of anti-PD-1 antibody treatment and that anti-CXCR2 monoclonal antibody therapy enhanced it (30,31). It has been reported that Sema4D induced MDSC in the tumor microenvironment (32) and that head and neck squamous cell carcinoma patients with high plasma Sema4D levels had less infiltration of immune cells into the tumor microenvironment (33). Experiments with murine oral cancer-1 showed that Sema4D Ab combined with either CTLA-4 or PD-1 blockade enhanced tumor rejection or delayed tumor growth (34). Such combination therapy that inhibits MDSCs may be effective for urothelial cancer.

The PCA algorithm can compress a dataset onto a lower-dimensional feature subspace to maintain the most relevant information. Therefore, PCA analysis was performed to characterize the immunological changes in various immune phenotypes caused by PEM. In fact, the results of Fig. 2 were summarized in Fig. 3. Irrespective of the pre-treatment chemotherapy, PCA demonstrated the T cells changes in PC1 and PC2. In addition, there were no statistically significant differences in the changes of immune cells, especially T cells, before and after PEM between patients who received >6 courses of chemotherapy vs. those who received ≤6 courses (Table SIX). Therefore, taken together, we considered PEM caused these T cell changes. In contrast, changes in mMDSC were affected by pre-treatment chemotherapy (Fig. S3).

There are several limitations to this study. First, the difficulties in accurately detecting all PD-1 receptors on T cells from patients treated with anti-PD-1 antibodies create a potential confounder because detecting antibodies compete for their binding to PD-1 with therapeutic antibodies (16). There are two major anti-PD-1 monoclonal antibodies, EH12.2H7 and MIH4. The former is more sensitive than the latter in the absence of PEM; however, EH12.2H7 competes for PD-1 binding with PEM and cannot detect PD-1 expression in the presence of PEM. On the other hand, MIH4 can bind to PD-1 in the presence of PEM; however, it only detects a part of PD-1 expression. We chose clone EH12.2H7; therefore, only the data before PEM administration can be evaluated. A similar problem might be observed in the previous report by Tzeng, reporting that anti-PD-L1 treatment correlated with decreased PD-L1$^+$ mMDSC, while doses of anti-PD-1 correlated with decreased PD-1$^+$ mMDSCs (35). A reliable method for quantifying PD-1 expression on immune cells from treated patients is warranted. Second, we only analyzed the immune cell changes before and after the first dose to identify predictive biomarkers for PEM response early during treatment. Therefore, data were difficult to represent the long-term changes in immune cells after PEM. The examination of the long-term changes of immune cells after PEM is required in future studies. Third, the type, timing, and dose of chemotherapy before administration of PEM was not unified in the present study. However, the changes in immune cell count between pre- and on-treatment samples were not affected by the number of chemotherapy courses (Table SIX). Finally, only patients whose peripheral blood could be collected twice, before and 3 weeks after starting PEM administration, were surveyed, which may have biased selection.

In conclusion, PEM treatment promoted the accumulation of CD4$^+$ and CD8$^+$ T cells with a senescent or late-differentiated phenotype and reduced the number of eTreg cells in the PB of UC patients. T cell activation is necessary for effective therapy, but excessive differentiation of T cells may be harmful for long-term survival. Changes in mMDSCs after PEM were different from those of other immune cells and their decrease in individual patients was associated with better overall survival.

Acknowledgements

The authors would like to thank Ms. Mikiko Shibuya and Ms. Yaeko Furuhashi (Department of Immunotherapeutics, The University of Tokyo Hospital, Tokyo, Japan) for processing blood samples. The authors would also like to thank Dr Ken-ichi Hashimoto (Department of Urology, The University of Tokyo Hospital, Tokyo, Japan) for collecting blood samples.

Funding

No funding was received.

Availability of data and materials

The datasets used and/or analyzed during the current study are available from the corresponding author on reasonable request.

Authors' contributions

TTe processed the blood samples and carried out the flow cytometry and biological analyses. YKo, YKu and KN designed the study, provided technical guidance and analyzed the data. TK, JM, YA, YY, YS and DY explained and obtained consent forms, collected peripheral blood samples, and analyzed and interpreted the data. NT and TTs provided guidance on statistical analysis and analyzed the data. KK and HK contributed conceptional design, interpreted the data, and confirmed the authenticity of all the raw data and the analysis results. TTe and KK wrote and revised the manuscript. All authors read and approved the final manuscript.

Ethics approval and consent to participate

This clinical study on the immunological impact of immunotherapy in patients with UC was conducted at The University of Tokyo Hospital. All procedures in this study were performed following the ethical standards of the institution, and in conformity with the 1964 Helsinki Declaration and its later amendments or comparable ethical standards. The research protocol was approved by the Ethical Committee of The University of Tokyo (Tokyo, Japan). Written informed consent to participate in the study was obtained from each patient before they entered the study.

Patient consent for publication

Patient consent for publication was covered by the informed consent document.

Competing interests

The authors declare that they have no competing interests.

References

1. Bellmunt J, de Wit R, Vaughn DJ, Fradet Y, Lee JL, Fong L, Vogelzang NJ, Climent MA, Petrylak DP, Choueiri TK, *et al*: Pembrolizumab as second-line therapy for advanced urothelial carcinoma. N Engl J Med 376: 1015-1026, 2017.
2. Yarchoan M, Hopkins A and Jaffee EM: Tumor Mutational Burden and response rate to PD-1 inhibition. N Engl J Med 377: 2500-2501, 2017.
3. Rosenberg JE, Hoffman-Censits J, Powles T, van der Heijden MS, Balar AV, Necchi A, Dawson N, O'Donnell PH, Balmanoukian A, Loriot Y, *et al*: Atezolizumab in patients with locally advanced and metastatic urothelial carcinoma who have progressed following treatment with platinum-based chemotherapy: A single-arm, multicentre, phase 2 trial. Lancet 387: 1909-1920, 2016.
4. Bagley SJ, Kothari S, Aggarwal C, Bauml JM, Alley EW, Evans TL, Kosteva JA, Ciunci CA, Gabriel PE, Thompson JC, *et al*: Pretreatment neutrophil-to-lymphocyte ratio as a marker of outcomes in nivolumab-treated patients with advanced non-small-cell lung cancer. Lung Cancer 106: 1-7, 2017.
5. Riedl JM, Barth DA, Brueckl WM, Zeitler G, Foris V, Mollnar S, Stotz M, Rossmann CH, Terbuch A, Balic M, *et al*: C-reactive protein (CRP) levels in immune checkpoint inhibitor response and progression in advanced non-small cell lung cancer: A Bi-center study. Cancers (Basel) 12: 2319, 2020.
6. Weide B, Martens A, Hassel JC, Berking C, Postow MA, Bisschop K, Simeone E, Mangana J, Schilling B, Di Giacomo AM, *et al*: Baseline biomarkers for outcome of melanoma patients treated with pembrolizumab. Clin Cancer Res 22: 5487-5496, 2016.
7. Kagamu H, Kitano S, Yamaguchi O, Yoshimura K, Horimoto K, Kitazawa M, Fukui K, Shiono A, Mouri A, Nishihara F, *et al*: $CD4^+$ T-cell immunity in the peripheral blood correlates with response to anti-PD-1 therapy. Cancer Immunol Res 8: 334-344, 2020.
8. Mazzaschi G, Facchinetti F, Missale G, Canetti D, Madeddu D, Zecca A, Veneziani M, Gelsomino F, Goldoni M, Buti S, *et al*: The circulating pool of functionally competent NK and $CD8^+$ cells predicts the outcome of anti-PD1 treatment in advanced NSCLC. Lung Cancer 127: 153-163, 2019.
9. Ornstein MC, Diaz-Montero CM, Rayman P, Elson P, Haywood S, Finke JH, Kim JS, Pavicic PG Jr, Lamenza M, Devonshire S, *et al*: Myeloid-derived suppressors cells (MDSC) correlate with clinicopathologic factors and pathologic complete response (pCR) in patients with urothelial carcinoma (UC) undergoing cystectomy. Urol Oncol 36: 405-412, 2018.
10. Jones BR, Miller RL, Kinloch NN, Tsai O, Rigsby H, Sudderuddin H, Shahid A, Ganase B, Brumme CJ, Harris M, *et al*: Genetic diversity, compartmentalization, and age of HIV proviruses persisting in $CD4^+$ T cell subsets during long-term combination antiretroviral therapy. J Virol 94: e01786-19, 2020.
11. Bronte V, Brandau S, Chen SH, Colombo MP, Frey AB, Greten TF, Mandruzzato S, Murray PJ, Ochoa A, Ostrand-Rosenberg S, *et al*: Recommendations for myeloid-derived suppressor cell nomenclature and characterization standards. Nat Commun 7: 12150, 2016.
12. Miyara M, Yoshioka Y, Kitoh A, Shima T, Wing K, Niwa A, Parizot C, Taflin C, Heike T, Valeyre D, *et al*: Functional delineation and differentiation dynamics of human $CD4^+$ T cells expressing the FoxP3 transcription factor. Immunity 30: 899-911, 2009.
13. Subramanian A, Kuehn H, Gould J, Tamayo P and Mesirov JP: GSEA-P: A desktop application for gene set enrichment analysis. Bioinformatics 23: 3251-3253, 2007.
14. Angelova M, Charoentong P, Hackl H, Fischer ML, Snajder R, Krogsdam AM, Waldner MJ, Bindea G, Mlecnik B, Galon J and Trajanoski Z: Characterization of the immunophenotypes and antigenomes of colorectal cancers reveals distinct tumor escape mechanisms and novel targets for immunotherapy. Genome Biol 16: 64, 2015.
15. Cassetta L, Fragkogianni S, Sims AH, Swierczak A, Forrester LM, Zhang H, Soong DYH, Cotechini T, Anur P, Lin EY, *et al*: Human tumor-associated macrophage and monocyte transcriptional landscapes reveal cancer-specific reprogramming, biomarkers, and therapeutic targets. Cancer Cell 35: 588-602.e10, 2019.
16. Zelba H, Bochem J, Pawelec G, Garbe C, Wistuba-Hamprecht K and Weide B: Accurate quantification of T-cells expressing PD-1 in patients on anti-PD-1 immunotherapy. Cancer Immunol Immunother 67: 1845-1851, 2018.
17. Mariathasan S, Turley SJ, Nickles D, Castiglioni A, Yuen K, Wang Y, Kadel EE III, Koeppen H, Astarita JL, Cubas R, *et al*: TGFβ attenuates tumour response to PD-L1 blockade by contributing to exclusion of T cells. Nature 554: 544-548, 2018.
18. Wei SC, Levine JH, Cogdill AP, Zhao Y, Anang NAS, Andrews MC, Sharma P, Wang J, Wargo JA, Pe'Er D and Allison JP: Distinct cellular mechanisms underlie anti-CTLA-4 and anti-PD-1 checkpoint blockade. Cell 170: 1120-1133.e17, 2017.
19. Shyer JA, Flavell RA and Bailis W: Metabolic signaling in T cells. Cell Res 30: 649-659, 2020.
20. Janelle V, Neault M, Lebel MÈ, De Sousa DM, Boulet S, Durrieu L, Carli C, Muzac C, Lemieux S, Labrecque N, *et al*: $p16^{INK4a}$ regulates cellular senescence in PD-1-expressing human T cells. Front Immunol 12: 698565, 2021.
21. Ruhland MK and Alspach E: Senescence and immunoregulation in the tumor microenvironment. Front Cell Dev Biol 9: 754069, 2021.
22. Francisco LM, Salinas VH, Brown KE, Vanguri VK, Freeman GJ, Kuchroo VK and Sharpe AH: PD-L1 regulates the development, maintenance, and function of induced regulatory T cells. J Exp Med 206: 3015-3029, 2009.
23. Bagchi S, Yuan R and Engleman EG: Immune checkpoint inhibitors for the treatment of cancer: Clinical impact and mechanisms of response and resistance. Annu Rev Pathol 16: 223-249, 2021.

24. Limagne E, Richard C, Thibaudin M, Fumet JD, Truntzer C, Lagrange A, Favier L, Coudert B and Ghiringhelli F: Tim-3/galectin-9 pathway and mMDSC control primary and secondary resistances to PD-1 blockade in lung cancer patients. Oncoimmunology 8: e1564505, 2019.
25. Dumitru CA, Moses K, Trellakis S, Lang S and Brandau S: Neutrophils and granulocytic myeloid-derived suppressor cells: Immunophenotyping, cell biology and clinical relevance in human oncology. Cancer Immunol Immunother 61: 1155-1167, 2012.
26. Hou A, Hou K, Huang Q, Lei Y and Chen W: Targeting myeloid-derived suppressor cell, a promising strategy to overcome resistance to immune checkpoint inhibitors. Front Immunol 11: 783, 2020.
27. Vincent J, Mignot G, Chalmin F, Ladoire S, Bruchard M, Chevriaux A, Martin F, Apetoh L, Rébé C and Ghiringhelli F: 5-Fluorouracil selectively kills tumor-associated myeloid-derived suppressor cells resulting in enhanced T cell-dependent anti-tumor immunity. Cancer Res 70: 3052-3061, 2010.
28. Wang Z, Till B and Gao Q: Chemotherapeutic agent-mediated elimination of myeloid-derived suppressor cells. Oncoimmunology 6: e1331807, 2017.
29. Li W, Zhang X, Chen Y, Xie Y, Liu J, Feng Q, Wang Y, Yuan W and Ma J: G-CSF is a key modulator of MDSC and could be a potential therapeutic target in colitis-associated colorectal cancers. Protein Cell 7: 130-140, 2016.
30. Highfill SL, Cui Y, Giles AJ, Smith JP, Zhang H, Morse E, Kaplan RN and Mackall CL: Disruption of CXCR2-mediated MDSC tumor trafficking enhances anti-PD1 efficacy. Sci Transl Med 6: 237ra67, 2014.
31. Li T, Liu T, Zhu W, Xie S, Zhao Z, Feng B, Guo H and Yang R: Targeting MDSC for immune-checkpoint blockade in cancer immunotherapy: Current progress and new prospects. Clin Med Insights Oncol: Aug 5, 2021 (Epub ahead of print).
32. Younis RH, Han KL and Webb TJ: Human head and neck squamous cell carcinoma-associated semaphorin 4D induces expansion of myeloid-derived suppressor cells. J Immunol 196: 1419-1429, 2016.
33. Younis RH, Ghita I, Elnaggar M, Chaisuparat R, Theofilou VI, Dyalram D, Ord RA, Davila E, Tallon LJ, Papadimitriou JC, *et al*: Soluble Sema4D in plasma of head and neck squamous cell carcinoma patients is associated with underlying non-inflamed tumor profile. Front Immunol 12: 596646, 2021.
34. Clavijo PE, Friedman J, Robbins Y, Moore EC, Smith E, Zauderer M, Evans EE and Allen CT: Semaphorin4D inhibition improves response to immune-checkpoint blockade via attenuation of MDSC recruitment and function. Cancer Immunol Res 7: 282-291, 2019.
35. Tzeng A, Diaz-Montero CM, Rayman PA, Kim JS, Pavicic PG Jr, Finke JH, Barata PC, Lamenza M, Devonshire S, Schach K, *et al*: Immunological correlates of response to immune checkpoint inhibitors in metastatic urothelial carcinoma. Target Oncol 13: 599-609, 2018.